Pressure-induced metallization of silane

Xiao-Jia Chen*†, Viktor V. Struzhkin*, Yang Song*‡, Alexander F. Goncharov*, Muhtar Ahart*, Zhenxian Liu*, Ho-kwang Mao*§, and Russell J. Hemley*§

*Geophysical Laboratory, Carnegie Institution of Washington, Washington, DC 20015; †School of Physics, South China University of Technology, Guangzhou 510641, China; and ‡Department of Chemistry, The University of Western Ontario, London, ON, Canada N6A 5B7

Contributed by Russell J. Hemley, November 6, 2007 (sent for review September 29, 2007)

There is a great interest in electronic transitions in hydrogen-rich materials under extreme conditions. It has been recently suggested that the group IVa hydrides such as methane (CH_4), silane (SiH_4), and germane (GeH_4) become metallic at far lower pressures than pure hydrogen at equivalent densities because the hydrogen is chemically compressed in group IVa hydride compounds. Here we report measurements of Raman and infrared spectra of silane under pressure. We find that SiH_4 undergoes three phase transitions before becoming opaque at 27–30 GPa. The vibrational spectra indicate the material transforms to a polymeric (framework) structure in this higher pressure range. Room-temperature infrared reflectivity data reveal that the material exhibits Drude-like metallic behavior above 60 GPa, indicating the onset of pressure-induced metallization.

high pressure | hydrogen-rich materials

As the lightest and putatively simplest of the elements, hydrogen forms a diatomic molecular gas at ambient conditions. In 1935, Wigner and Huntington (1) first predicted that molecular hydrogen would undergo a transition to a metallic state under sufficiently strong compression. Metallic hydrogen is also predicted to be superconducting with a high transition temperature (2, 3). Studies of hydrogen have long been a major driving force in high-pressure science and technology development and remain an important challenge in modern physics and astrophysics (4). Shock-compressed fluid hydrogen reported to be metallic at 140 GPa and 3000 K based on measurements of electrical conductivity (5), but the experimental realization of metallic hydrogen in the solid form has remained elusive (6–8). Nevertheless, there has been remarkable progress in the study of other low-Z systems at high density, including the discovery of superconductivity in lithium at high pressures with a transition temperature as high as 20 K (9–11).

Ashcroft (12) has suggested that the dense hydrides of group IVa elements (C, Si, Ge, and Sn) would undergo a transition to eventual metallic and superconducting state at pressures considerably lower than may be necessary for solid hydrogen because hydrogen has already been compressed in these hydride compounds. Recent theoretical studies predict that silane (SiH_4) (13–15), germane (GeH_4) (16), and stannane (SnH_4) (17) metallize at much lower and accessible pressures. However, surprisingly little information is available about the high-pressure behavior of these heavy group IVa hydrides (18, 19). An insulator to semiconductor transition for solid SiH_4 was reported at 100 GPa from reflectivity data at visible wavelengths (18). Synchrotron x-ray diffraction measurements (19) showed that the crystal structure of SiH_4 in the pressure range between 10 and 25 GPa is monoclinic with space group $P2_1/c$, and four molecules in the unit cell. Until now, there has been no report on the metallization in the group IVa hydrides. It is therefore of interest to explore their metallic phases at high pressures.

Here we present measurements of Raman and synchrotron infrared spectroscopy of solid SiH_4 in diamond anvil cells up to 70 GPa. We find that, after passing through four phase transition, solid SiH_4 undergoes major changes in optical properties in the visible range at 27–30 GPa. The infrared spectra reveal an increase in reflectivity starting at 60 GPa indicative of pressure-induced metallization. Therefore, SiH_4 can be considered as the first example for the metallization of a group IVa hydride.

Results

Vibrational spectroscopy is crucial for characterizing high-pressure phase transformation of low-Z molecular materials. The symmetry of the isolated SiH_4 molecule is T_d; therefore, it has four normal vibrational modes. These are labeled $\nu_1(A_1)$, $\nu_2(E)$, $\nu_3(F_2)$, and $\nu_4(F_2)$, all of which exhibit Raman activity, whereas only the two F_2 modes are infrared active. In the fluid phase (98 K), ν_2 appears at 961.7 cm^{-1} in the Raman spectrum, whereas the $\nu_3 \approx \nu_1$ bands cannot be entirely resolved due to overlap of the Raman bands in this region and possible partial mixing of the two modes (20). The ν_4 band at 881.7 cm^{-1} in the fluid SiH_4 has been detected by infrared measurements (20, 21). We have measured the Raman spectra of SiH_4 at room temperature and various pressures up to 31.6 GPa. The results up to 2,400 cm^{-1} are shown in Fig. 1. For low-pressure fluid SiH_4, the observed spectrum agrees well with previous experiments (20–22).

We observed multiplet spectra at both low and high frequencies above 4 GPa. Both the profile and relative intensities of the multiplet spectra change markedly at higher pressures. Lattice phonons with low intensity are observed below 500 cm^{-1} in the solid and pressure shifts them to higher frequencies. The ν_2 bands at $\approx$900 cm^{-1} are characteristic of vibrations associated with Si—H bending and the high-frequency bands $\nu_3 - \nu_1$ at 2,200 cm^{-1} can be assigned to Si—H bond stretching. The multiplicity of components for the observed fundamental indicates that there is more than one molecule per primitive unit cell in solid SiH_4. Structure studies (19) showed that SiH_4 has a monoclinic phase with $P2_1/c$ symmetry between 10 and 25 GPa, with four molecules in the unit cell. SiH_4 thus has 60 vibrational modes in the Brillouin zone center. The symmetries of these modes are $15A_g + 15A_u + 15B_g + 15B_u$, where $A_u + 2B_u$ are acoustic modes and the rest are optic modes, the g modes exhibit Raman activity, whereas the u modes are infrared active. Among them, 12 are translational, including the acoustic modes mentioned above, 12 are rotational, and the rest are internal modes. Each fundamental correlates with modes of all symmetries in broad agreement with the observed spectra. The number of the observed modes is smaller than the number predicted because some are either not observed or nearly degenerate.

At atmospheric pressure, solid SiH_4 crystallizes in two low-temperature phases, with a transition temperature at 63.8 K from the fluid to phase I (21) and the second phase appearing at 38 K (I-II) (22). All of our measured spectra are entirely different from those of phase I and II (20), indicating that SiH_4 transforms

Author contributions: X.-J.C., V.V.S., H.-k.M., and R.J.H. designed research; X.-J.C., V.V.S., Y.S., A.F.G., M.A., Z.L., H.-k.M., and R.J.H. performed research; X.-J.C., V.V.S., and A.F.G. analyzed data; and X.-J.C., V.V.S., A.F.G., H.-k.M., and R.J.H. wrote the paper.

The authors declare no conflict of interest.

§To whom correspondence may be addressed. E-mail: h.mao@gl.ciw.edu or r.hemley@gl.ciw.edu.

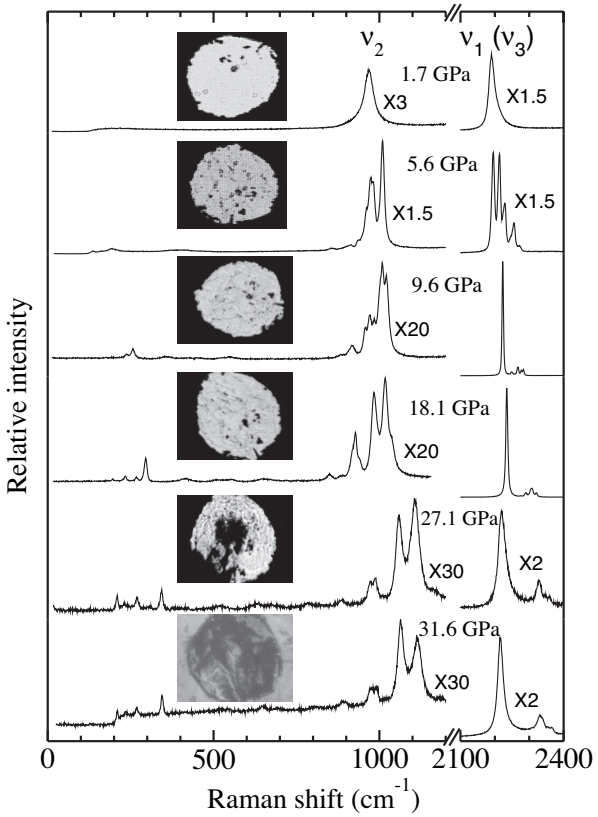

Fig. 1. Raman spectra of various high-pressure phases of SiH_4 at room temperature: 1.7 GPa, fluid; 5.6 GPa, solid phase III; 9.6 GPa, phase IV; 18.1 GPa, phase V; 27.1 GPa, phases V+VI; 31.6 GPa, phase VI. Photomicrographs in the center column are views through the diamond windows of the pressure cell (sample diameter, ≈200 μm). At 27.1 GPa, the center portion of the sample turns into the opaque (but still nonmetallic) phase VI. At 31.6 GPa, the totally opaque sample indicates completion of transition to phase VI.

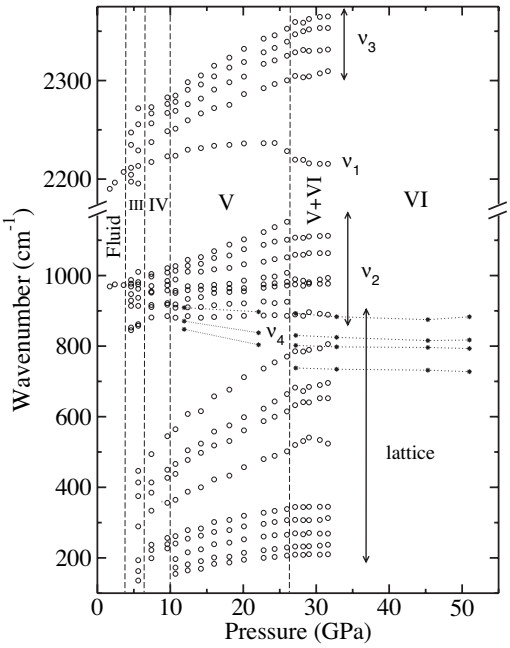

Fig. 2. Pressure-induced frequency shifts of Raman (open circles) and infrared (filled circles) active vibrations of SiH_4 at room temperature. The vertical dashed lines at 4.0, 6.5, 10.0, and 26.5 GPa indicate the phase boundaries.

to new phases. Photomicrographic images of samples taken at various pressures can be used to determine the phase boundaries. On freezing at 1.7 GPa at room temperature, SiH_4 was observed to be transparent and colorless. Solid–fluid phase transition occurs at ≈4.0 GPa. The color of the solid phases remains unchanged over a wide pressure range. However, the samples begin to become black in transmission at ≈27 GPa and the black portions extend gradually as pressure is increased. The entire samples are observed to turn completely opaque at 31.6 GPa. Two solid phases therefore coexist during the color change to black. Sun *et al.* (18) reported that SiH_4 remains transparent in the pressure range 7–92 GPa. Our measurements were highly reproducible. We observed changes in optical properties at 27–30 GPa in six experimental runs. Moreover, our Raman data below 27 GPa clearly can be fully understood based on our obtained structural symmetry. We observed the changes in optical properties at 27–30 GPa in six experimental runs.

Vibrational frequencies provide information on the high-pressure behavior (Fig. 2). Four high-pressure solid phases are detected, which we designate as phases III, IV, V, and VI. Above 4 GPa, SiH_4 enters a solid phase III from its fluid state. A discontinuity in the Raman-active ν_1, ν_2, and ν_3 modes occurs at 6.5 GPa on going from phase III to IV. A solid-solid phase transition at 10 GPa from phase IV to phase V is identified based on a change of the number of Raman-active lattice bands. When solid SiH_4 becomes black above 26.5 GPa, three major Si—H bending ν_2 modes disappear. Meanwhile, pressure causes a decrease in the frequency of the ν_1 band in phase VI. These rich features across the V–VI phase boundary at 26.5 GPa and line broadening of most modes beyond that indicate a change in the structure of SiH_4. It should be noted that no Raman bands were observed for the highest-pressure phase, which appears above 32 GPa. The result excludes a decomposition to atomic (metallic) Si and molecular H_2.

Fig. 3 shows high-pressure reflectivity spectra of solid SiH_4 from 600 to 8,000 cm^{-1}. The data were corrected for the absorption by the diamonds. At all pressures, we observed fringes arising from interference between parallel surfaces in the pressure cell from ruby particles bridged between the diamond anvils. An important observation is the systematic increase in the

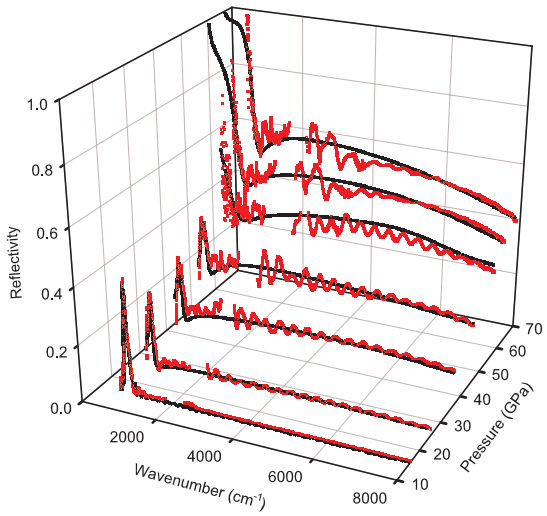

Fig. 3. Room-temperature infrared reflectivity spectra of SiH_4 at selected pressures up to 67.2 GPa. The red squares are the measurements. The solid lines represent model fits to the data. The small gap in the spectrum near 2,000 cm^{-1} is due to diamond anvil absorption. The oscillations are interference fringes caused by the anvils.

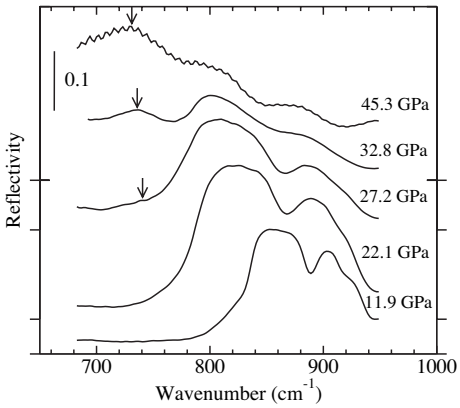

Fig. 4. Infrared reflectivity spectra of SiH_4 in the Si—H bending region. The tick labels on the reflectivity axis denote zero reflectivity at each pressure. The spectra are offset with the exception of the spectra at 32.8 and 45.3 GPa have the same zero point. The arrows indicate the appearance of new fundamental modes when the SiH_4 sample becomes opaque.

reflectivity with pressure over most of the frequency range studied. The low-pressure data exhibit sharp ν_4 bands in the low-frequency region (see Fig. 4). The frequencies of these bands decrease with increasing pressure. As pressure is increased above 60 GPa, the low-frequency bands become weaker in the reflectivity spectra concomitant with a significant rise in reflectivity in the infrared. The reflectivity is above 80% down to 600 cm^{-1}.

Discussion

The reflectivity results provide spectroscopic evidence for the pressure-induced metallization in solid SiH_4. The reflectivity is given by $R = |r|^2 = |N - n_d|^2/|n + n_d|^2$, where $N = n + ik$ is the complex refractive index and n_d is the refractive index of diamond for measurements in a diamond cell. The reflectivity coefficient $r(\omega) = |r(\omega)|\exp[i\theta(\omega)]$ has amplitude $|r(\omega)|$ and phase $\theta(\omega)$ components. In general, a material has characteristic resonant frequencies due to lattice vibrations and oscillations of the bound electrons within the atoms. The real and imaginary parts of the complex dielectric function ($\varepsilon = \varepsilon_1 + i\varepsilon_2 \equiv N^2$) can be fit to the reflectivity data (23)

$$\varepsilon(\omega) = \varepsilon_\infty + \sum_{j=1}^{m} \frac{\omega_{pj}^2}{\omega_j^2 - \omega^2 - i\omega\gamma_j}, \qquad [1]$$

where ω_j and γ_j are the frequency and damping terms of a particular resonance line, ω_{pj} is the plasma frequency, and ε_∞ is the real part of the limiting dielectric constant. The results of the fits of the reflectivity data are also shown by the solid lines in Fig. 3.

We see that the model accounts for the general shape of the spectrum, indicating that solid SiH_4 is metallic when the pressure is >60 GPa. The obtained ω_p is 1.20×10^4 and 1.54×10^4 cm^{-1} for 60.7 and 67.2 GPa, respectively.** These values are in the frequency range of metallic Pb at ambient conditions. The high-pressure spectra of SiH_4 show a broad absorption at high frequencies, which could be the result of a pressure-induced interband transition. As pressure increases, the broad absorption gradually increases. Similar behavior has been found for high-pressure metallic solid oxygen (24). Although the reflectivity spectrum of SiH_4 is complex. The analysis thus indicates the onset of Drude-type behavior diagnostic of metallization at 60 GPa. A significant increase in reflectivity takes place on a low energy side, shifting with increasing pressure to high energies, as expected in a free electron metal.

We now compare these results with various theoretical predictions. Metallization of SiH_4 was first predicted to take place at 91 GPa in the *Pman* structure (13). Yao *et al.* (14) predicted that a metallic monoclinic phase with *C*2/*c* symmetry is dynamically stable at 90 and 125 GPa. They interpreted the insulator–metal transition to be associated with the transformation from a molecular to a polymeric phase with bridging hydrogens. Our observed pressure of metallization is close to, but lower than, these theoretical values. Meanwhile, Pickard and Needs (15) found that the predicted metallic *C*2/*c* phase becomes stable at 263 GPa, below which pressure an insulating phase having $I4_1/a$ symmetry remains the lowest enthalpy phase down to 50 GPa. In a powder x-ray diffraction study (25), $I4_1/a$ was considered as a possible space group for a body-centered tetragonal structure of phase II. The Raman spectra reveal that all high-pressure phases up to 31.6 GPa differ from phase II.

Infrared reflectivity spectra of solid SiH_4 in the Si—H bending regime are shown in Fig. 4. Three phonon bands near ≈850 cm^{-1} are observed and soften with increasing pressure. At 27 GPa, a new soft phonon mode at ≈738 cm^{-1} appears and grows in intensity and softens with increasing pressure. Combining this information with the disappearance of three ν_2 bands as well as the frequency decline of the ν_1 band in phase VI supports a major change in structure before the transition to a metallic phase, which has been confirmed by x-ray diffraction (19). Additional x-ray data suggest a structural change. The structure and electronic properties above 60 GPa require further investigation. Fig. 2 also summarizes the evolution of the phonon bands with pressure. As can be seen, low-frequency lattice modes cross the bending Si—H modes near 27 GPa in the vicinity of the V–VI transition. This clearly shows that phase VI is not molecular. The color of the sample also changes remarkably at the transition from phase V to VI, suggesting a large decrease of the band gap energy. Therefore, both the structural phase transition and band gap closure contribute to the pressure-induced metallization of SiH_4.

Conclusions

High-pressure spectroscopy has been used to characterize the high-pressure behavior of silane. We find from Raman spectroscopy the fluid–solid transition at ≈4.0 GPa and three solid-solid transitions near 6.5, 10, and 26.5 GPa at room temperature (above which the material becomes opaque at 27–30 GPa). Infrared spectra more clearly show the character of the 26.5 GPa transition. The infrared results show an increase in reflectivity starting at 60 GPa, signaling pressure-induced metallization. Soft modes could be important if metallic SiH_4 eventually becomes a superconductor under pressure. Measurements of the electrical resistivity and higher pressure diffraction measurements will provide additional insight into this possibility.

Materials and Methods

SiH_4 gas (99.998%; Aldrich) was loaded in diamond anvil cells with rhenium gaskets in a glove box. Sample loadings were done by precooling the chamber in liquid nitrogen, with ruby grains for measuring pressure from the R_1 luminescence line (26). Once SiH_4 was trapped under pressure in the sample chamber, the cells were warmed to room temperature for the optical experiments. Raman spectra were measured in a backscattering geometry, with an argon ion laser for excitation. The collimated laser beam was focused with an estimated power on the sample of <25 mW. The Raman spectra were analyzed by a single-stage spectrograph with a multichannel CCD detector. Synchrotron infrared spectra were collected at the U2A beamline at the National Synchrotron Light Source of Brookhaven National Laboratory. The areas of the samples illuminated were 15 μm in diameter. The system has a Bruker IFS 66v/S vacuum Fourier transform interferometer and Bruker IRscope-II microscope equipped with a nitrogen cooled HgCdTe type-A detector. All spectra were obtained at room temperature with a resolution of 4 cm^{-1}.

**The model parameters are: at 60.7 GPa, $n_d = 2.38$, $\varepsilon_\infty = 8.0$, $\gamma_1 = 384$ cm^{-1}, $\omega_{p2} = 7.20 \times 10^4$ cm^{-1}, $\omega_2 = 6.70 \times 10^3$ cm^{-1}, and $\gamma_2 = 9.20 \times 10^3$ cm^{-1}; at 67.2 GPa, $n_d = 2.38$, $\varepsilon_\infty = 8.0$, $\gamma_1 = 94.86$ cm^{-1}, $\omega_{p2} = 8.36 \times 10^4$ cm^{-1}, $\omega_2 = 4.87 \times 10^3$ cm^{-1}, and $\gamma_2 = 9.19 \times 10^3$ cm^{-1}.

ACKNOWLEDGMENTS. We thank J. Xu and S. A. Gramsch for helpful discussions and J. S. Tse and C. R. Rotundu for reviewing the manuscript and for their comments. This work was supported by Office of Basic Energy Sciences Grant DEFG02-02ER3495, National Nuclear Security Administration of the U.S. Department of Energy Grant DEFC03-03NA00144, and U.S. National Science Foundation Grant DMR-0205899. The National Synchrotron Light Source, Brookhaven National Laboratory, is supported by the U.S. Department of Energy, Office of Science, Office of Basic Energy Sciences, under Contract DE-AC02-98CH10886.

1. Wigner E, Huntington HB (1935) On the possibility of a metallic modification of hydrogen. *J Chem Phys* 3:764–770.
2. Ashcroft NW (1968) Metallic hydrogen: A high-temperature superconductor. *Phys Rev Lett* 21:1748–1749.
3. Richardson CF, Ashcroft NW (1997) High temperature superconductivity in metallic hydrogen: Electron-electron enhancements. *Phys Rev Lett* 78:118–121.
4. Ginzburg VL (2004) Nobel Lecture: On superconductivity and superfluidity (what I have and have not managed to do) as well as on the ''physical minimum'' at the beginning of the XXI century. *Rev Mod Phys* 76:981–998.
5. Weir ST, Mitchell AC, Nellis WJ (1996) Metallization of fluid molecular hydrogen at 140 GPa (1.4 Mbar). *Phys Rev Lett* 76:1860–1863.
6. Mao HK, Hemley RJ (1989) Optical studies of hydrogen above 200 gigapascals: Evidence for metallization by band overlap. *Science* 244:1462–1465.
7. Goncharov AF, Gregoryanz E, Hemley RJ, Mao HK (2001) Spectroscopic studies of the vibrational and electronic properties of solid hydrogen to 285 GPa. *Proc Natl Acad Sci USA* 98:14234–14237.
8. Loubeyre P, Occelli F, LeToullec R (2002) Optical studies of solid hydrogen to 320 GPa and evidence for black hydrogen. *Nature* 416:613–617.
9. Shimizu K, Ishikawa H Takao D, Yagi T, Amaya K (2002) Superconductivity in compressed lithium at 20 K. *Nature* 419:597–599.
10. Struzhkin VV, Eremets MI, Gan W, Mao HK, Hemley RJ (2002) Superconductivity in dense lithium. *Science* 298:1213–1215.
11. Deemyad S, Schilling JS (2003) Superconducting phase diagram of Li metal in nearly hydrostatic pressures up to 67 GPa. *Phys Rev Lett* 91:167001.
12. Ashcroft NW (2004) Hydrogen dominant metallic alloys: High temperature superconductors. *Phys Rev Lett* 92:187002.
13. Feng J, Grochala W, Jaroń T, Hoffmann R, Bergara A, Ashcroft NW (2006) Structures and potential superconductivity in SiH_4 at high pressure: En route to ''metallic hydrogen.'' *Phys Rev Lett* 96:017006.
14. Yao Y, Tse JS, Ma Y, Tanaka K (2007) Superconductivity in high-pressure SiH_4. *Europhys Lett* 78:37003.
15. Pickard CJ, Needs RJ (2006) High-pressure phases of silane. *Phys Rev Lett* 97:045504.
16. Martinez-Canales M, Bergara A, Feng J, Grochala W (2006) Pressure induced metallization of germane. *J Phys Chem Solids* 67:2095–2099.
17. Tse JS, Yao Y, Tanaka K (2007) Novel superconductivity in metallic SnH_4 under high pressure. *Phys Rev Lett* 98:117004.
18. Sun LL, Ruoff AL, Zha CS, Stupian G (2006) High pressure studies on silane to 210 GPa at 300 K: Optical evidence of an insulator–semiconductor transition. *J Phys Condens Matter* 18:8573–8580.
19. Degtyareva O, Martinez-Canales M, Bergara A, Chen XJ, Song Y, Struzhkin VV, Mao HK, Hemley RJ (2007) Crystal structure of SiH_4 at high pressure. *Phys Rev B* 76:064123.
20. Fournier RP, Savoie R, The ND, Belzile R, Cabana A (1972) Vibrational-spectra of SiH_4 and SiD_4-SiH_4 mixtures in condensed states. *Can J Chem* 50:35–42.
21. Clusius K (1933) Free rotation in the lattice of monosilane. *Z Phys Chem B* 23:213–225.
22. Wilde RE, Srinivasan TKK (1975) Detection of phase-transitions in heavy silane by ir spectroscopy. *J Phys Chem Solids* 36:119–122.
23. Barker AS, Jr (1964) Transverse and longitudinal optic mode study in MgF_2 and ZnF_2. *Phys Rev A* 136:1290–1295.
24. Desgreniers S, Vohra YK, Ruoff AL (1990) Optical-response of very high-density solid oxygen to 132 GPa. *J Phys Chem* 94:1117–1122.
25. Sears WM, Morrison JA (1975) Solid SiH_4: Structure and orientational order. *J Chem Phys* 62:2736–2739.
26. Mao HK, Xu JA, Bell PM (1986) Calibration of the ruby pressure gauge to 800 kbar under quasi-hydrostatic conditions. *J Geophys Res* 91:4673–4676.